

Creation of classical and quantum fluxons by a current dipole in a long Josephson junction

Boris A. Malomed

Department of Interdisciplinary Studies,

Faculty of Engineering,

Tel Aviv University

Tel Aviv 69978, Israel

Alexey V. Ustinov

Physikalisches Institut III, Universität

Erlangen-Nürnberg

D-91058, Erlangen, Germany

(Dated: March 22, 2022)

Abstract

We study static and dynamical properties of fluxons in a long annular Josephson junction (JJ) with a current injected at one point and collected back at a close point. Uniformly distributed dc bias current with density γ is applied too. We demonstrate that, in the limit of the infinitely small size of the current dipole, the critical value of γ , above which static phase distributions do not exist, that was recently found (in the Fraunhofer's analytical form) for the annular JJ with the length much smaller than the Josephson penetration length, is valid irrespective of the junction's length, including infinitely long JJs. In a long annular JJ, the dipole generates free fluxon(s) if γ exceeds the critical value. For long JJs, we also find another critical value (in an analytical form too), which is always slightly smaller than the Fraunhofer value, except for points where the dipole strength is $2\pi N$ with integer N , and both values vanish. The static phase configuration which yields the new critical value is based on an unstable fluxon-antifluxon bound state, therefore it will probably not manifest itself in the usual (classical) regime. However, it provides for a dominating *instanton* configuration for tunnel birth of a free fluxon, hence it is expected to determine a quantum-birth threshold for fluxons at ultra-low temperatures. We also consider the interaction of a free fluxon with the complex consisting of the current dipole and antifluxon pinned by it. A condition for suppression of the net interaction force, which makes the long JJ nearly homogeneous for the free fluxon, is obtained in an analytical form. The analytical results are compared with numerical simulations. The analysis presented in the paper is relevant to the recently proposed new experimental technique of inserting fluxons into annular Josephson junctions.

PACS numbers: 74.50.+r, 85.25.-j, 03.65.Xp

INTRODUCTION

Long Josephson junctions (JJs) are well known to be a unique physical system that allows one to experimentally study dynamics of topological solitons in the form of fluxons (alias Josephson vortices, each carrying a magnetic-flux quantum Φ_0) [1, 2]. For both experimental and theoretical studies, the most convenient object is an *annular* (circular) long JJ, in which the net number of initially trapped fluxons is conserved, hence new solitons may only be created as fluxon-antifluxon pairs [3, 4]. Fluxon dynamics in the annular junctions manifests itself in the clearest way, as it is not complicated by reflections from boundaries. The interest to annular long JJs stems from the great potential they offer for fundamental studies of dynamical properties of solitons, such as, e.g., emission of the Cherenkov radiation [5, 6]. A challenging problem for the theory is quantum soliton dynamics in long JJs, which has been recently observed in experiment at ultra-low temperatures [7]. On the other hand, annular JJs offer applications in cryoelectronics, such as sources of highly coherent microwave radiation [4] and radiation detectors [8]. Besides that, long annular JJs have a potential for designing fluxon qubits [9, 10] and fluxon ratchets [11, 12].

A key problem in experiments with annular JJs is the trapping of a desired number of fluxons. The only previously known method which made it possible to do that in a controllable way is rather complicated, relying upon the use of a scanning electron (or laser) microscope [13]. Other studies relied on fluxon trapping in the course of cooling the system below the critical temperature T_c of the superconducting electrodes [3, 4, 5, 6, 14, 15]. However, the latter technique does not provide for reproducible results, and requires heating of the junction to high temperatures. Moreover, trapped fluxons generated in such a manner get often pinned by Abrikosov vortices, which may be trapped in the electrodes in the course of cooling below T_c .

In a recent work [16], a new method to insert fluxons into annular JJs was proposed and demonstrated experimentally and numerically. It is based on injecting a relatively large current I into the junction locally; the current flows from the injection point into the superconducting electrode and also across the Josephson barrier, and is collected back at another point of the same electrode, which is separated from the injection spot by a small distance D . The schematic view of such JJ is given in Fig. 1. In the following, we use the normalized notation for the distance between the current injectors, $d = D/\lambda_J$, and the

current, $\varepsilon = I/\lambda_J$, where λ_J is the Josephson penetration depth.

In this setting, one is actually dealing with a *current dipole*, the total current traversing the Josephson barrier being zero. The dipole gives rise to a local magnetic flux Φ in the region between the injection and collection points. If the magnitude of this pinned flux attains the flux quantum Φ_0 , it may become energetically favorable (in the presence of an additional dc bias current uniformly distributed along the junction) to have the pinned flux compensated by a negative flux $-\Phi_0$. In fact, this implies that a fluxon-antifluxon pair is created in the annular JJ, so that the antifluxon carrying the flux $-\Phi_0$ is pinned by the current dipole, while elsewhere in the long junction there appears a free fluxon carrying the compensating flux Φ_0 . Further, if Φ exceeds $N\Phi_0$, then N free fluxons are expected to appear in the annular JJ.

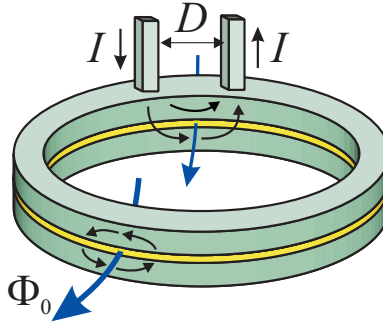


FIG. 1: A sketch of the annular Josephson junction with a current dipole formed by local injection of current I into one of the superconducting electrodes.

One objective of this work is to theoretically analyze the above problem and find a critical condition for the generation of free fluxons by the current dipole in a long JJ biased by the uniformly distributed dc bias current γ . Results will be obtained in an exact analytical form (in section II) for the case when the dipole strength $\kappa \equiv \varepsilon d$ is finite, while $d \rightarrow 0$ and $\varepsilon \rightarrow \infty$. Two different solutions will be obtained. One of them yields a critical value of γ which coincides with the Fraunhofer expression (see below), that was recently found as a condition for the transition into a resistive state in a short annular JJ, whose full length was assumed to be much smaller than λ_J [17]. In our solution, the length of the ring junction may be arbitrarily large. Thus, we demonstrate that the Fraunhofer formula for the critical bias current is a *universal* one, which is valid irrespective of the dipole strength and junction's length.

The second analytical solution reported in this paper is exact only for long junctions. It yields the critical value of γ which is slightly smaller than the one given by the first solution. However, the configuration on which the second solution is based (essentially, it is a fluxon-antifluxon bound state) is, plausibly, always unstable. For this reason, the second solution may be irrelevant to the experimental technique outlined above in the usual (classical) regime of operation. However, precisely this second solution defines an *instanton* [18] which controls the tunneling rate for quantum birth of a free fluxon, in the same long JJ, at ultra-low temperatures. The instanton predicts that the exponentially small factor, which limits the quantum-birth rate, will scale as a square root of that for the long uniform junction, i.e., the quantum yield is strongly enhanced by the current dipole. Therefore, the second solution is physically meaningful too. The analytical predictions will be compared with results of direct numerical simulations of the critical condition (in the classical situation).

A free fluxon moving in the annular JJ will periodically collide with the antifluxon pinned by the current dipole and the dipole itself. An important issue is to minimize interaction between the free fluxon and the dipole-antifluxon complex, so that the junction would seem as uniform as possible for the moving soliton. In section III, we demonstrate, in an approximate analytical form, that, keeping the dipole size d and current ε finite (or proceeding to the limit of the point-wise dipole), one may indeed select their values so that the interaction is strongly suppressed. This prediction, which has immediate relevance to the experiment, is also compared with direct numerical simulations.

CRITICAL CONDITIONS FOR GENERATION OF FREE CLASSICAL AND QUANTUM FLUXONS

General considerations

The system outlined above is described by the following perturbed sine-Gordon (sG) equation for the superconducting phase difference ϕ , which is written in the standard notation [1, 2]:

$$\begin{aligned} \phi_{tt} - \phi_{xx} + \sin \phi = \\ -\alpha \phi_t - \gamma - \varepsilon [\delta(x - d/2) - \delta(x + d/2)], \end{aligned} \tag{1}$$

where δ is the Dirac delta-function [it is used in Eq. (1) due to the assumption, which corresponds to the experimental situation, that the injection and collection leads have their width much smaller than λ_J], γ is the density of the uniformly distributed dc bias current, and α is a dissipative constant. In the limit of the point-like dipole ($d \rightarrow 0$), the limiting form of Eq. (1) is

$$\phi_{tt} - \phi_{xx} + \sin \phi = -\alpha \phi_t - \gamma + \kappa \delta'(x), \quad (2)$$

where $\kappa \equiv \varepsilon d$ is the dipole strength defined above, and δ' is the derivative of the delta-function.

The model (2) has been first studied almost two decades ago by Aslamazov and Gurovich [19]. These authors considered interaction of fluxons with an Abrikosov vortex trapped in one of the junction's electrodes, so that the vortex' normal core is parallel to the tunnel barrier. Later, the influence of the Abrikosov vortex on the fluxon bound states localized near the junction boundary was studied by Fistul and Giuliani [20].

In the special case $\kappa = \pi$, Eq. (2) is also used as a model which describes composite long JJs including segments of 0-type and π -type Josephson barriers [21]. Such composite junctions can be fabricated, for example, by using zigzag barriers between s -wave and d -wave superconductors [22]. This model gives rise to stable semi-fluxons (π -fluxons with a semi-integer topological charge). As it was pointed out by Goldobin *et al.* [21], semi-fluxons can also be created in a conventional long junction with local current injection in the form of a current dipole.

The critical condition for the transition to a free moving fluxon is defined in the following way: it is necessary to find a maximum value γ_{\max} of the bias current density γ such that, for given κ , static (time-independent) solutions to Eq. (2) exist for $|\gamma| < \gamma_{\max}$, and do not exist if $|\gamma|$ exceeds γ_{\max} . As it was clearly shown by dint of direct simulations of Eq. (1) reported in Ref. 16, the disappearance of the static solution means the appearance of freely moving fluxon(s) in the long JJ.

Double integration of the static version ($\phi_t = 0$) of Eq. (2) in a vicinity of the point $x = 0$ yields the following boundary conditions (b.c.) to be satisfied at this point:

$$\phi(x = +0) - \phi(x = -0) = \kappa; \quad \phi'(x = +0) = \phi'(x = -0). \quad (3)$$

Off the point $x = 0$, the static solution obeys the equation

$$-\phi'' + \sin \phi + \gamma = 0. \quad (4)$$

Further analysis of the static problem based on Eqs. (3) and (4) will be presented in the next subsection.

In the sG system operating in the quantum regime (i.e., in a long JJ kept at extremely low temperatures), fluxon-antifluxon pairs can be produced as a result of under-barrier tunneling [23]. The corresponding tunneling rate is determined by an instanton solution, which starts with some static field configuration (which is just a flat phase distribution, in the case of a homogenous system) and, going in imaginary time under the energy barrier, ends up on the physical shell, with a state consisting of far separated fluxon and antifluxon. It was shown that, in the presence of local inhomogeneities, the quantum birth of fluxon-antifluxon pairs may be facilitated (the corresponding tunneling rate being enhanced by an exponentially large factor) if one or both solitons appear on the *mass shell* (appear as real quasi-particles after completion of the tunneling) in a state pinned by an inhomogeneity [24]. In this connection, it is important to find a threshold γ_{thr} (a minimum value of γ) past which there appears a state with a pinned fluxon and free antifluxon, i.e., an effective threshold for the quantum birth of fluxons in the quantum regime. A difference from the problem of finding the above-mentioned value γ_{max} , which determines the threshold for the creation of a free fluxon in the classical regime, is that, on the way from $\gamma = 0$ to $\gamma = \gamma_{\text{max}}$, the corresponding static solutions to Eq. (2) need not be stable; just on the contrary, instanton solutions usually go through unstable states, such as fluxon-antifluxon pairs, as the evolution in imaginary time does not require stability in real time [23, 24].

Critical current in the annular junction of arbitrary length, the classical regime

In the case of a finite-length annular JJ, the above-mentioned static problem takes the following form: one should find a solution to Eq. (4) such that it satisfies b.c. which is tantamount to Eq. (3):

$$\phi(x = L) - \phi(x = 0) = \kappa; \quad \phi'(x = L) = \phi'(x = 0), \quad (5)$$

where L is the full length of the annular junction. Irrespective of the length, Eq. (2) is equivalent to the Newton's equation of motion in "time" x for a particle with the coordinate ϕ , in the presence of the potential

$$U(\phi) = -\gamma\phi + \cos\phi, \quad (6)$$

hence the motion conserves the Hamiltonian,

$$H = \frac{1}{2} \left(\frac{d\phi}{dx} \right)^2 + \cos \phi + \gamma \phi. \quad (7)$$

In the annular junction of any length, the values of H on both sides of the matching point, $x = 0$, must be equal, as they belong to one and the same solution. Besides that, due to the continuity of $d\phi/dx$ at the matching point $x = 0$, see Eqs. (3), the values of $(d\phi/dx)^2$ are also equal on both sides. Thus, equating the values of the Hamiltonian, we obtain a condition

$$\cos(\phi_1 + \kappa) + \gamma(\phi_1 + \kappa) = \cos \phi_1 + \gamma \phi_1, \quad (8)$$

where ϕ_1 is the value on ϕ on one left side of the matching point, the value on the right side being $\phi_2 = \phi_1 + \kappa$, according to Eqs. (3).

A more convenient form of Eq. (8) is

$$\gamma = \kappa^{-1} [(1 - \cos \kappa) \cos \phi_1 + (\sin \kappa) \sin \phi_1]. \quad (9)$$

One can now look for the largest possible value of the expression on the right-hand side of Eq. (9) that can be obtained by varying ϕ_1 . This yields an expression of the Fraunhofer's type for the critical bias-current density,

$$\gamma_c = 2\kappa^{-1} \sin(\kappa/2), \quad (10)$$

which is attained at $\phi_1 = \pi/2 - \kappa/2$.

Thus, Eq. (10) gives the largest value of γ beyond which no static solution may exist in a vicinity of the point dipole in the annular JJ of any length, implying a transition to a dynamical regime, i.e., generation of free fluxon(s) in the case of the long JJ. Note, however, that it may happen that more than one critical values exist, then Eq. (10) gives, according to its derivation from Eq. (9), only the *largest* one among them. In fact, it will be shown in the next subsection that (in the case of the long JJ) there indeed exists exactly one more critical value, which is smaller than (10), see Eq. (13) below.

Quite naturally, in the limit $\kappa \rightarrow 0$ Eq. (10) yields $\gamma_c = 1$, which is the commonly known critical value of the bias current density in the long homogeneous JJ [1]. The fact that γ_c vanishes at $\kappa = 2\pi$ is also easy to understand: the static equation (4) has obvious stable uniform solutions,

$$\phi_0^{(n)} = -\sin^{-1} \gamma + 2\pi n \quad (11)$$

(provided that $|\gamma| \leq 1$), with an arbitrary integer n , hence the b.c. (3) with $\kappa = 2\pi$ implies that two such solutions, $\phi_0^{(0)}$ and $\phi_0^{(1)}$, match to each other across the point $x = 0$; in the annular system, they must be connected by a static 2π -kink, which is possible exactly at $\gamma = 0$. Similarly, in the case $\kappa = 2\pi N$ with any integer N , Eq. (10) again yields $\gamma_c = 0$, which means that N fluxons will appear spontaneously in this case, without the application of the bias current.

The result (10) *does not* depend on the length of the annular junction; for this reason, it coincides with the threshold for transition to a resistive state in a *short* annular JJ, which was found in the recent work [17]. It is relevant to mention that the actual calculation of the threshold in that work was performed in an altogether different way, so that the sG equation was not used at all.

The fluxon-birth threshold in the long annular junction, the quantum regime

Coming back to the case of the long JJ, we note that a solution for $\phi(x)$ must assume the background value (11) (for instance, with $n = 0$) far from the dipole (formally, at $x \rightarrow \pm\infty$). Thus, in the case of a very long (formally, infinite) junction, we need to find two solutions of Eq. (4), in the regions, respectively, $x > 0$ and $x < 0$, so that one solution assumes the asymptotic value (11) at $x \rightarrow +\infty$, and the other one assumes the same value at $x \rightarrow -\infty$. The solutions must be matched at the point $x = 0$, pursuant to b.c. (3), and it is necessary to find a maximum value of $|\gamma|$ for which the matching is possible with a given dipole strength κ .

Consideration of the equivalent mechanical problem mentioned above, i.e., motion in the potential (6), demonstrates that there are *exactly two* solutions to this problem. One of them yields the above result (10). A description of both solutions (for the case of a very long JJ) is given below.

Both solutions employ the single function $\phi(x)$ which satisfies Eq. (4) and assumes the same asymptotic value (11) simultaneously at $x \rightarrow +\infty$ and $x \rightarrow -\infty$. This function represents a fluxon-antifluxon (ff) bound state; it is an even function, with a maximum value ϕ_{\max} at the central point. Using the conservation of the Hamiltonian (7), one can find a relation between ϕ_{\max} and ϕ_0 , which takes the form

$$\gamma \sin^{-1} \gamma + \cos(\sin^{-1} \gamma) = -\gamma \phi_{\max} + \cos \phi_{\max}. \quad (12)$$

In addition to the $\bar{f}\bar{f}$ solution, Eq. (4) also has a semi-divergent one, which starts with the value (11), say, at $x = -\infty$, and diverges as $\phi(x) \approx (\gamma/2)x^2$ at $x \rightarrow +\infty$. This solution may also be employed to construct a full static state consisting of two pieces that are matched as per Eqs. (3) at $x = 0$. It is easy to check that the state built as the combination of the $\bar{f}\bar{f}$ and semi-divergent solutions disappears, with the increase of γ , exactly at the critical point (10), so this is how the solution corresponding to the Fraunhofer's formula (10) looks in the long JJ.

Besides this matched state, there is another one, specific to the long junction. It can be constructed from two pieces belonging to the $\bar{f}\bar{f}$ solution [it is easy to see that no state satisfying the b.c. (3) can be constructed if both pieces belong to the semi-divergent solution; thus no extra solution is possible in addition to the two presently considered ones].

At the critical point corresponding to the disappearance of the new matched state, the b.c. (3) are satisfied in an extreme form: on one side of the point $x = 0$, we have the uniform background solution, $\phi \equiv \phi_0$, while on the other side a piece of the $\bar{f}\bar{f}$ solution is to be used. Due to the continuity of the derivative $\phi'(x)$ at $x = 0$ [see Eqs. (3)] and the fact that ϕ' vanishes at the matching point in the critical case [as the derivative of $\phi(x) \equiv \phi_0$ is zero], the central point (the one with $\phi = \phi_{\max}$) of the $\bar{f}\bar{f}$ solution, which is the only spot where the derivative vanishes, must be set exactly at $x = 0$ when one attains the critical configuration, see Fig. 2. In view of the first b.c. (3), this means that the background value (11) and ϕ_{\max} are related (in the critical state) so that $\phi_{\max} = \kappa + \phi_0 \equiv \kappa - \sin^{-1} \gamma$. This expression should be inserted in Eq. (12). After that, the “worst” transcendental terms $\gamma \sin^{-1} \gamma$ in the ensuing equation mutually cancel, and the remaining equation can be solved in an exact form, to yield a new critical value of γ , which, this time, we call a threshold one:

$$\gamma_{\text{thr}} = \frac{2 \sin^2(\kappa/2)}{\sqrt{4 \sin^4(\kappa/2) + (\kappa - \sin \kappa)^2}}. \quad (13)$$

As well as in the case of the Fraunhofer expression (10), the limit value of γ_{thr} for $\kappa \rightarrow 0$ is 1, which is the above-mentioned critical bias-current density in the uniform long JJ. On the other hand, if κ is close to 2π , i.e., the phase jump in b.c. (3) is close to 2π , the $\bar{f}\bar{f}$ solution takes the form of a bound state of a fluxon and an antifluxon separated by a large distance, which implies that even a small bias current is able to destroy this configuration pinned by the dipole. Accordingly, one finds from Eq. (13) that

$$\gamma_{\text{thr}} \approx (4\pi)^{-1} (\kappa - 2\pi)^2 \quad (14)$$

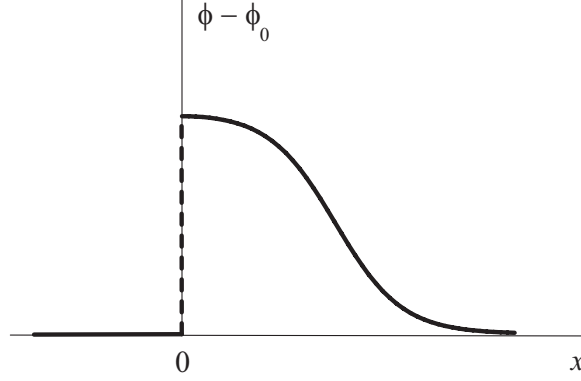


FIG. 2: A sketch of the critical field configuration that gives rise to the threshold value (13) of the bias-current density.

when κ is close to 2π , which should be compared to the asymptotic form of the Fraunhofer critical value in the same case: as it follows from Eq. (10), $|\gamma_c| \approx |\kappa - 2\pi|/8$. On the contrary to this linearly vanishing expression, Eq. (14) shows that the newly found threshold value vanishes quadratically. As well as the Fraunhofer critical value, the threshold one (14) has higher-order minima at $\kappa = 2\pi N$ with N integer.

The comparison of the two critical values (versus κ) is shown below as a part of Fig. 4(a). As is seen from the figure (and can be proved analytically), the threshold value (14) is always smaller (except for the points $\kappa = 2\pi N$, where both critical values vanish), which implies that, in the application to the tunnel-birth problem for fluxons in the quantum system, it will be a dominating one. In principle, for the same reason it could play a dominant role in the transition to the dynamical regime in the classical case, but, in fact, this is hindered by the instability of the $\bar{f}\bar{f}$ static configuration which underlies Eq. (13). Unlike this, it was checked in direct simulations that the configuration based on the matched $\bar{f}\bar{f}$ and semi-divergent solutions, which yields the Fraunhofer's expression (10), is always stable in the long junction (for the case $\kappa = \pi$, it was also shown in Ref. [25]). However, as it was explained above, the dynamical instability of the intermediate state does not bar using the configuration as a part of the under-barrier instanton trajectory.

While detailed consideration of the under-barrier production of fluxons in the quantum system is beyond the scope of this work, we briefly mention that the above-mentioned instanton may be constructed, following the pattern of the critical configuration that yields the threshold value (13), as precisely a *half* of the fluxon-antifluxon bound state on one side of

the point $x = 0$, matched to the uniform state (11) on its other side. This makes the integral of the system's action, taken along the under-barrier evolution in the imaginary time, which determines the exponential smallness of the tunneling rate [23], equal to exactly half the integral in the absence of the current dipole. For this reason, the exponential smallness is expected to scale as the *square root* of that in the uniform system, so that the tunneling will be strongly enhanced. As for the direct role of the threshold value (13), it implies that, if γ is taken larger than it, the tunneling mechanism will directly generate a free fluxon in the system.

SUPPRESSION OF THE INTERACTION BETWEEN A FREE FLUXON AND THE ANTIFLUXON PINNED BY THE CURRENT DIPOLE

As it was mentioned in the Introduction, another problem relevant to the experiment is to suppress interaction between an already existing free fluxon and its antifluxon counterpart, which is pinned by the dipole pair of currents in the long JJ. A natural way to select parameters of the dipole configuration in Eq. (1) with, generally speaking, *finite* d and ε , so that to minimize the interaction, is to consider the case when the distance between the free fluxon and pinned antifluxon is large enough, so that the interaction between them may be treated by means of the perturbation theory [26]. In the framework of this approach, the free fluxon with zero velocity, whose form is

$$\phi_{\text{fl}} = 4 \tan^{-1} [\exp (\sigma(x - \xi))] , \quad (15)$$

where ξ is the coordinate of the fluxon's center, and $\sigma = \pm 1$ is its polarity, is regarded as a quasi-particle. Since the term in the Hamiltonian of the full sG model (1), which corresponds to the current-dipole terms in the equation, is $H_{\text{dip}} = \varepsilon [\phi(x = d/2) - \phi(x = -d/2)]$, it is easy to obtain an effective potential of direct interaction of the free fluxon with the current dipole, substituting the waveform (15) in H_{dip} . Eventually, one can find an effective force of the direct fluxon-dipole interaction,

$$\begin{aligned} F_{\text{dip}} &\equiv -\frac{dH_{\text{dip}}}{d\xi} = 2\sigma\varepsilon [\text{sech}(\xi - d/2) - \text{sech}(\xi + d/2)] \\ &\approx 8\sigma\varepsilon \sinh(d/2) e^{-\xi}, \end{aligned} \quad (16)$$

where we made use of the assumption that the distance $|\xi|$ of the fluxon from the dipole is large. The polarity σ of the free fluxon and the sign of the current ε must correlate so that

the free fluxon is repelled by the dipole, while the corresponding antfluxon is attracted by the it (otherwise, the antfluxon cannot be in the pinned state). As it follows from Eq. (16), this implies that $\sigma = \text{sign } \varepsilon$.

Besides that, the fluxon also interacts with the antfluxon pinned by the dipole. A well-known perturbative expression for the interaction force between the fluxon and antfluxon is [26] $F_{\text{antifl}} \approx -32 e^{-\xi}$. Then, a simple condition for the effective suppression of the net interaction between the free fluxon and the complex including the current dipole and the antfluxon pinned by it may be formulated as a condition for mutual cancellation of the two forces, the repulsive one F_{dip} and the attraction force F_{antifl} , which produces the following result:

$$|\varepsilon| \sinh(d/2) = 4. \quad (17)$$

The meaning of this result is that the free fluxon is expected to move nearly as in the homogeneous long JJ if the parameters of the current dipole are selected according to Eq. (17). Note also that, in the limit of the point-like dipole, which was dealt with in the previous section, i.e., $\varepsilon \rightarrow \infty$ and $d \rightarrow 0$, the condition (17) takes a very simple form, $\kappa = 8$. This result is obtained in the framework of the approximations adopted above, but it is not very different from the exact result that follows from Eq. (10), i.e., $\kappa = 2\pi$ (at this value of κ , the fluxon can be very easily separated from the dipole-antfluxon complex).

The validity of the prediction (17) was checked against direct numerical simulations of the full equation (1). For instance, in the case shown below in Fig. 5, with $\varepsilon = 8$ and $d = 0.5$, the product on the left-hand side of Eq. (17) takes the value 4.17, and the interaction with the dipole-antfluxon complex indeed gives rise to a very small perturbation in motion of the free fluxon. Simulation run for values of $|\varepsilon| \sinh(d/2)$ quite different from 4 (not shown here, as the pictures are rather messy) demonstrate a much stronger perturbation.

NUMERICAL SIMULATIONS

In order to verify analytical results for the fluxon injection, we performed numerical simulations by solving the full equation (1). In the simulations, each δ -function in Eq. (1) was approximated by its smooth counterpart,

$$\varepsilon \delta(x) \approx \eta g(x) \equiv \eta \text{sech}^2(2x/\xi), \quad (18)$$

such that $\eta\xi = \varepsilon$, which complies with the definition $\int_{-\infty}^{+\infty} \delta(x)dx = 1$. This approximation implies that the injected current is spread over the distance $\simeq \xi\lambda_J$. We will present results obtained with the values $\xi = 1$ and $\xi = 0.1$, which lie in a typical experimentally accessible range of this parameter [16]. The numerically calculated current-voltage characteristics will be shown in normalized units as $\gamma(v)$, where v is the average fluxon velocity normalized to the Swihart velocity \bar{c} . With this normalization $v = 1$ corresponds to the asymptotic voltage of the single-fluxon step. The simulations are performed with the normalized junction length $L = 10$ and dissipation coefficient $\alpha = 0.1$.

Figure 3(a) presents the calculated dependence of the critical current γ_c on the injection-current amplitude ε for $d = 2$. The inset shows the adopted approximation for the injected-current profile, $f(x) = \eta[g(x - d/2) - g(x + d/2)]$, see Eq. (18), with $\xi = 1$ and $\eta = 9$. As it has already been concluded from experimental data [16], the dependence in Fig. 3 is very similar to the conventional Fraunhofer pattern of the critical current in a small Josephson junction in the magnetic field, the length of the equivalent small junction being associated with the distance d between the injecting points. The overlap between the lobes gets larger for larger d . Due to this overlap, the minimum value of the critical (fluxon-depinning) current between the lobes decreases with d .

Numerically calculated I - V curves for various values of the injection current (indicated in the plots) are shown in Fig. 3(b). One-fluxon and two-fluxon steps can be clearly recognized here. Numerical data show that the steps on I - V curves are accounted for by fluxons freely moving under the action of the uniformly distributed bias current. It can be noted from Fig. 3(a) that there is a residual pinning of fluxon(s) due to the disturbance produced by the current injectors. This pinning is smallest at injection-current values which lie between the lobes of the $\gamma_c(\varepsilon)$ curve. Thus, for a given injector spacing d , the residual fluxon pinning can be minimized by choosing an appropriate value for the injection current ε .

In order to numerically model the point-like dipole given by the last term of Eq. (2), we used the derivative $g'(x)$ of the function $g(x)$ defined by Eq. (18). Figure 4(a) shows the calculated dependence γ_c on the dipole-current amplitude κ . The inset shows the numerically used current profile, $f(x) \equiv \eta g'(x - d/2)$ with $\xi = 0.1$. The spatial grid used in this calculation had $\Delta x = 0.01$. In spite of the limited accuracy of our numerical scheme because of the sharp current profile, the agreement between the numerical data and the Fraunhofer formula (10), represented by the solid line, is very good. For the comparison's sake, in

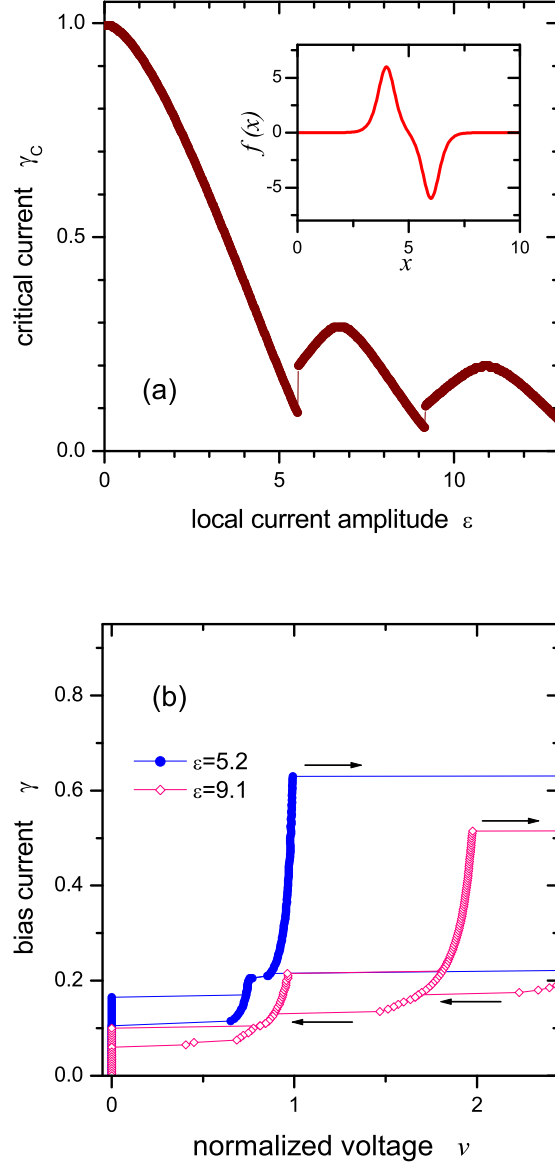


FIG. 3: (a) Numerically calculated dependence of the critical current of the annular junction γ_c on the injection-current amplitude ε for $d = 2$. (b) Numerically calculated current-voltage characteristics of the annular junction for two values of the injection current, $\varepsilon = 5.2$ and $\varepsilon = 9.1$.

Fig. 4(a) the dashed line shows the newly-found threshold value given by Eq. (13).

The numerically calculated I - V curves for the point-like dipole are shown in Fig. 4(b). In comparison with Fig. 3(b), the depinning current is very small, and the value of the bias-current density corresponding to the steps is very close to the maximum value, $\gamma = 1$. Both the one-fluxon and two-fluxon steps can be hardly distinguished from those in the ideal

uniform annular junction with trapped fluxons.

The presentation of numerical results is concluded by Fig. 5. It shows a 2D gray scale-plot of the spatially-temporal evolution of the instantaneous normalized voltage $\varphi_t(x, t)$ in the annular junction for $\varepsilon = 8$, $d = 1$, and $\gamma = 0.4$. The moving fluxon is recognized as a solitary-wave packet propagating at a nearly constant velocity across the junction. One can see that the disturbance of the fluxon motion in the region where the current injector is located is tiny, which was explained above, by the proximity of this case to the interaction-suppression condition (17). The residual perturbation may, nevertheless, be significant at small velocities of the fluxon, when its kinetic energy is comparable to the pinning potential generated by the perturbation.

CONCLUSION

In this work, we have considered static and dynamical solutions for fluxons in the model of the annular Josephson junction with the local current dipole. The analysis is relevant for interpreting the recent experiment [16] that implemented a new technique of inserting fluxons into long junctions.

Recently, a critical value of the bias-current density γ , above which the system performs transition to a dynamical state, was found [17], in the Fraunhofer's form, for annular junctions whose length is much smaller than λ_J . We have shown that, in the limit of the infinitely narrow current dipole, the same critical expression is valid *at all values* of the junction's length. In the long junction, the dipole generates free fluxon(s) when γ exceeds the critical value γ_c . We have also found another critical value γ_{thr} for long junctions, which is always slightly smaller than the Fraunhofer's one, except for points where both vanish. The phase configuration which yields the new critical value is generated by an unstable fluxon-antifluxon bound state, therefore it is not relevant to the classical-fluxon-generation regime. However, it determines a quantum-birth threshold for fluxons in the quantum regime. It was also concluded that these two critical values exhaust all possible solutions to the problem of finding the critical bias-current density in the presence of the current dipole.

The interaction of a free fluxon with the complex consisting of the current dipole and antifluxon pinned by it was considered too. A condition for suppression of the effective interaction force was predicted, which makes the long junction effectively uniform for the

motion of the free fluxon.

The analytical predictions obtained in this work were checked against direct simulations. In all the cases, they agree well.

ACKNOWLEDGEMENTS

We appreciate valuable discussions with E. Goldobin. B.A.M. acknowledges financial support from DAAD (Deutscher Akademischer Austauschdienst) and hospitality of the Physics Institute at the Universität Erlangen-Nürnberg.

-
- [1] A. Barone and G. Paternó, *Physics and Applications of the Josephson Effect* (Wiley: New York, 1982).
 - [2] A. V. Ustinov, *Physica D* **123**, 315 (1998).
 - [3] A. Davidson, B. Dueholm, B. Kryger, and N. F. Pedersen, *Phys. Rev. Lett.* **55**, 2059 (1985).
 - [4] A. Davidson, B. Dueholm, and N. F. Pedersen, *J. Appl. Phys.* **60**, 1447 (1986).
 - [5] E. Goldobin, A. Wallraff, N. Thyssen, and A. V. Ustinov, *Phys. Rev. B* **57**, 130 (1998).
 - [6] A. Wallraff, A. V. Ustinov, V. V. Kurin, I. A. Shereshevsky, and N. K. Vdovicheva, *Phys. Rev. Lett.* **84**, 151 (2000).
 - [7] A. Wallraff, A. Lukashenko, J. Lisenfeld, A. Kemp, Y. Koval, M. V. Fistul, and A. V. Ustinov, *Nature* **425**, 155 (2003).
 - [8] C. Nappi and R. Christiano, *Appl. Phys. Lett.* **70**, 1320 (1997); M. P. Lissitski et al., *Nucl. Instr. and Methods in Phys. Research A* **444**, 476 (2000).
 - [9] A. Wallraff, Y. Koval, M. Levitchev, M. V. Fistul, and A. V. Ustinov, *J. Low Temp. Phys.* **118**, 543 (2000).
 - [10] A. Kemp, A. Wallraff and A. V. Ustinov, *Phys. Stat. Sol.(b)* **233**, 472 (2002).
 - [11] E. Goldobin, A. Sterck, and D. Koelle, *Phys. Rev. E* **63**, 031111 (2001).
 - [12] G. Carapella, *Phys. Rev. B* **63**, 054515 (2001).
 - [13] A. V. Ustinov, T. Doderer, B. Mayer, R. P. Huebener, and V. A. Oboznov, *Europhys. Lett.* **19**, 63 (1992).
 - [14] I. V. Vernik, V. A. Oboznov, and A. V. Ustinov, *Phys. Lett. A* **168**, 319 (1992).

- [15] A. V. Ustinov, Pis'ma Zh. Eksp. Teor. Fiz. **64**, 178 (1996) [Sov. Phys. JETP Lett. **64**, 191 (1996)]; I. V. Vernik, S. Keil, N. Thyssen, T. Doderer, A. V. Ustinov, H. Kohlstedt, and R. P. Huebener. J. Appl. Phys. **81**, 1335 (1997); A. V. Ustinov, B. A. Malomed, and N. Thyssen, Phys. Lett. A **233**, 239 (1997).
- [16] A. V. Ustinov, Appl. Phys. Lett. **80**, 3153 (2002).
- [17] C. Nappi, M. P. Lissitski, and R. Cristiano, Phys. Rev. B **65**, 132516 (2002).
- [18] R. Rajaraman, *An Introduction to Solitons and Instantons in Quantum Field Theory* (Amsterdam: North Holland, 1982).
- [19] L. G. Aslamazov and E. V. Gurovich, Pis'ma Zh. Eksp. Teor. Fiz. **40**, 22 (1984) [Sov. Phys. JETP Lett. **40**, 746 (1984)].
- [20] M. V. Fistul and G. F. Giuliani, Phys. Rev. B **58**, 9343 (1998).
- [21] E. Goldobin, D. Koelle, and R. Kleiner, Phys. Rev. B **66**, 100508(R) (2002).
- [22] H. J. H. Smilde, Ariando, D. H. A. Blank, G. J. Gerritsma, H. Hilgenkamp, and H. Rogalla, Phys. Rev. Lett. **88**, 057004 (2002).
- [23] K. Maki, Phys. Rev. Lett. **39**, 46 (1977); Phys. Rev. B **18**, 1641 (1978).
- [24] I. V. Krive, B. A. Malomed, and A. S. Rozhavsky, Phys. Rev. B **42**, 273 (1990).
- [25] E. Goldobin, private communication.
- [26] Y. S. Kivshar and B. A. Malomed, Rev. Mod. Phys. **61**, 763 (1989).

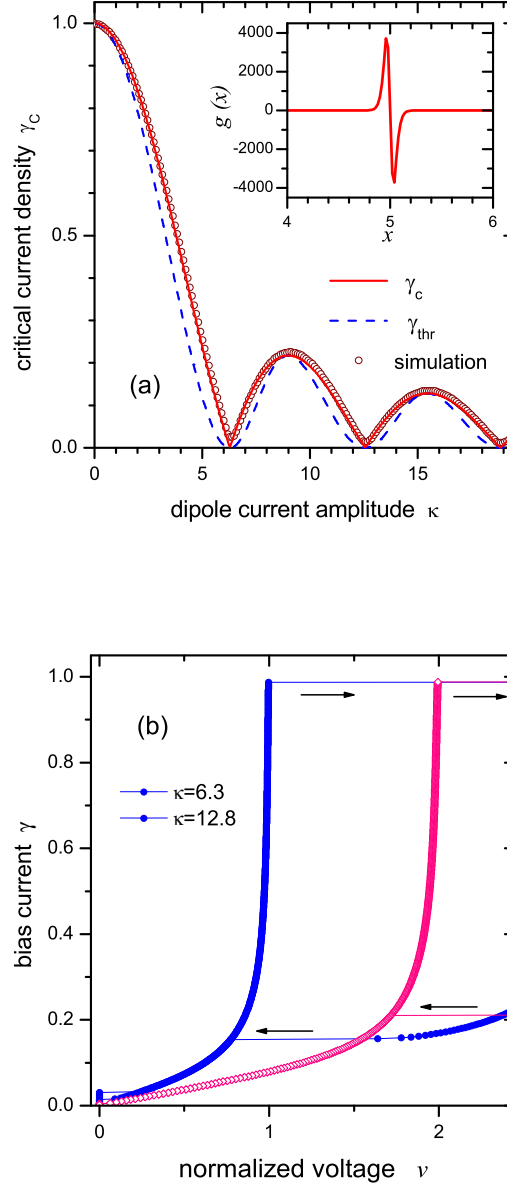


FIG. 4: (a) Numerically calculated dependence of the critical current in the annular junction, γ_c , on the dipole-current amplitude κ . The newly found threshold value, given by Eq. (13) (dashed line), and the Fraunhofer value, given by Eq. (10) (solid line) are included too. (b) Numerically calculated current-voltage characteristics of the annular junction for two values of the dipole's strength, $\kappa = 6.3$ and $\kappa = 12.8$.

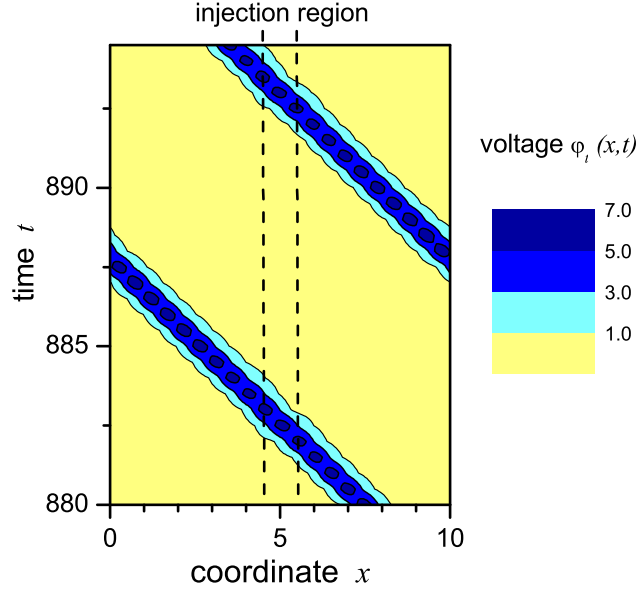


FIG. 5: Spatio-temporal evolution of the normalized instantaneous voltage in simulations of the annular Josephson junction with $\varepsilon = 8$, $d = 1$ and $\gamma = 0.4$. Dashed lines indicate the current injection points.